RSC Advances

This article can be cited before page numbers have been issued, to do this please use: X. Xiao, W. Zhu, Y. Lei, Q. Liu , Q. Li and W. Li, *RSC Adv.*, 2016, DOI: 10.1039/C6RA02979E.

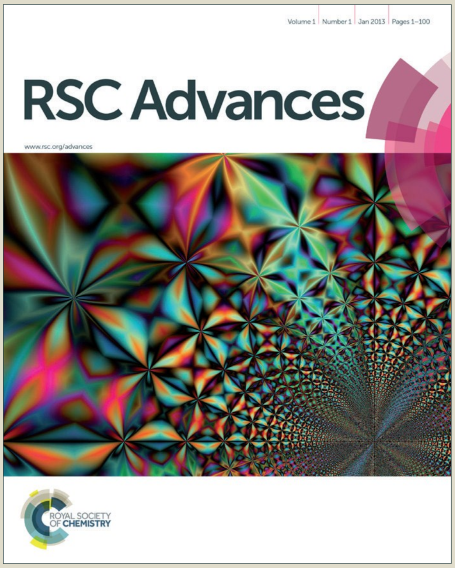

ROYAL SOCIETY OF CHEMISTRY

www.rsc.org/advances

View Article Online
DOI: 10.1039/C6RA02979E

Journal Name

ARTICLE

Zwitterionic buffer-induced visible light excitation of TiO_2 for efficient pollutant photodegradation

Received 00th January 20xx,
Accepted 00th January 20xx

DOI: 10.1039/x0xx00000x

www.rsc.org/

Xiang Xiao[a,b], Wen-Wen Zhu[a], Yu-Bin Lei[a], Qiu-Yue Liu[a], Qian Li[a], Wen-Wei Li[b,*]

Excitation of TiO_2 for visible light absorption by surface complexation with antenna organic molecules is an effective strategy to improve its solar utilization efficiency for photocatalytic application, but the existing antenna molecules are mostly toxic and environmentally-aggressive, severely limiting their practical application. In this study, we tested the potential of zwitterionic buffers (Good's buffers) as an environmentally-benign alternative. The addition of Good's buffers was found to significantly enhance methyl orange (MO) photodegradation by TiO_2 under visible light, but the enhancement degree varied with the different buffer types, buffer concentration and solution pH. The presence of 4-(2-hydroxyerhyl) piperazine-1-erhanesulfonic acid (HEPES) as a typical Good's buffer led to over 90% MO removal within 180 min, whereas only slight MO removal was observed in the TiO_2 alone system during the same period. Such an induced visible light photocatalytic activity was attributed to a complexation between the conjugate acid structured buffer molecule and TiO_2, which favors a ligand-to-metal charge transfer (LMCT). The LMCT activity was strongly dependent on the molecule structure, especially the states of hydroxyl and amino groups of Good's buffers. The pH buffering ability of the buffers also contributed to the efficient MO photodegradation. This study suggests a great potential of Good's buffers as both "green" antenna molecules and pH buffer for strengthening TiO_2-based photocatalytic remediation processes.

Introduction

TiO_2 has become the most widely investigated photocatalyst since the first discovery of its ability for photo-catalyzing water splitting in 1972.[1] It has many advantages such as low toxicity and cost, good water insolubility, hydrophilicity, chemical stability and resistance to photocorrosion. However, due to the large band gap (3.2 eV for anatase and brookite, 3.0 eV for rutile), the excitation wavelength of TiO_2 falls in the UV region,[2-4] which accounts for only 4-5% of the solar spectrum. To extend its photo response to the visible region, various strategies, such as metal ion/nonmetal ion doping, sensitizing by organic compounds or metal complexes, and noble metal deposition,[5-7] were explored. Surface modification by directly adding chemicals is considered as a promising methods to boost the photoreaction.[8] Especially, the ligand-to-metal charge transfer (LMCT) mediated pathway of TiO_2 under visible light has received intensive attentions.[9-13] Surface complexation of TiO_2 by some antenna organic molecules, such as aromatic organics, organic acids and amines that are commonly seen in the environment, confer it the ability of visible light absorption,[9-11] but most of these complexation agents are toxic and environmentally-aggressive.

Zwitterionic *N*-substituted aminosulfonic acids, first introduced by Good and co-workers,[14] are widely used as biological buffers in various reactions due to their nontoxicity, biocompatibility, weak complexation properties, and conveniently-controllable pKa values. The hydroxyl or amino functional groups of such zwitterionic buffers (or called Good's buffers) could induce LMCT excitation.[15-17] Thus, we hypothesize they may be used to enhance photocatalytic reactions by playing two roles: 1) serving as green antenna molecules to strengthen visible light adsorption by TiO_2; 2) to provide a favourable pH condition for photoexcitation of TiO_2.[18]

Here, we aim to validate the above hypothesis and explore the potential of Good's buffers as an enhancer of visible light photocatalytic processes. Five kinds of Good's buffers were tested as antenna molecules for TiO_2 nanoparticles, and the visible light activities of the corresponding complexes for methyl orange (MO) photodegradation were evaluated. In addition, the mechanisms of Good's buffer-induced visible light excitation of TiO_2 were investigated by using HEPES as a model buffer and evaluating the MO photodegradation performances under different buffer concentration and pH conditions. This work may have valuable implications for developing more efficient and sustainable photocatalytic processes for broad-range applications such as environmental remediation and renewable energy production.

Experimental

Chemicals

---

[a] School of The Environment and Safety Engineering, Jiangsu University, Zhenjiang, 212013, China
[b] CAS Key Laboratory of Urban Pollutant Conversion, Department of Chemistry, University of Science & Technology of China, Hefei 230026, China

† Electronic Supplementary Information (ESI) available: This section contains four figures. See DOI: 10.1039/x0xx00000x

View Article Online
DOI: 10.1039/C6RA02979E

Anatase TiO_2 nanoparticle used in this study were purchased from Wanjing New Material Co., China. The nanoparticles were found to be uniform with 25-nm average size (Fig. S1). The biological buffers (listed in Table 1) were purchased from Sangon Biotech Co., Ltd. (Shanghai, China).

Photodegradation Tests

The photocatalytic efficiency of TiO_2 was evaluated by using MO as a model pollutant. The reaction solution contained 10 mg L^{-1} MO, 500 mg L^{-1} TiO_2, and 50-mM Good's buffer. The solution pH was adjusted to 7.0 unless otherwise specified. The serum vials, each contained 20-ml mixed solution, were bubbled with N_2 for 20 min to remove the O_2, sealed with butyl rubber stoppers and then sonicated. All the serum vials were continuously stirred in the dark for 20 min on a shaker (200 rpm) to achieve adsorption-desorption equilibrium. Then, illumination with two incandescent lamps (60 W) was applied. Samples were collected during the reaction period and the MO concentration was monitored using a UV-vis spectrometer at 464 nm. The photocatalytic activity was quantitatively evaluated according to the equation:

$$\text{Residual rate}(\%) = \frac{C}{C_0} \times 100\%$$

where C_0 refers to the initial MO concentration and C represents the concentration at a given time during the photodegradation.

The influences of MO concentration (with gradients of 10, 20, 50 and 100 mM) and solution pH (6.5, 7.0, 7.5 and 8.0, adjusted with 1M NaOH) on the LMCT excitation of TiO_2-HEPES was evaluated. To elucidate the MO degradation pathway, ammonium oxalate (AO) and Cr(VI) were used as scavengers of holes (h^+)[19] and electrons (e^-),[20, 21] respectively.

Chemical analysis

The interaction between HEPES and TiO_2 was examined by UV-vis diffuse reflectance spectroscopy (DRS). TiO_2 suspensions (1.0 g L^{-1}) were buffered with 50 mM HEPES at pH 7.0, and stirred for overnight in the dark. After centrifugation at 6000 rpm for 10 min, the solids was collected and dried at room temperature. The DRS spectra were measured on a UV-2450 spectrometer (Shimadzu) equipped with an integrating sphere attachment, using $BaSO_4$ as background.

Agilent (Waldbronn, Germany) 6890N Series gas chromatograph equipped with a 7683B injector and a 5975B mass spectrometry detector was used to analyze the MO degradation products. The GC parameters were as follows: split ratio, 2:1; column, HP-5-MS capillary (30 m×0.25 mm I.D., 0.25 μm film thickness, Agilent, Waldbronn, Germany); injection port temperature, 220°C; carrier gas, helium; flow rate, 1.5 mL/min; oven temperature, initially 80°C for 3 min, ramped to 150°C at 10°C/min, 150°C for 5 min, and ramped to 250°C at 20°C/min, 250°C for 4 min. Before sample injection the sample solution was extracted by CH_2Cl_2. One microliter of extract was filtered through 0.22-μm membrane filter and then 1 μL of filtrate was injected into GC/MS for measurement.

Results and discussion

MO photodegradation with different Good's buffers

Photocatalytic efficiencies of TiO_2 for MO degradation in the absence or presence of different Good's buffers as antenna molecules were evaluated (Fig. 1). The buffer-free control showed only 10% MO removal after irradiation for 4 h, confirming a low photocatalytic activity of TiO_2 under visible light. This result also indicates that photosensitization was not a main cause of the MO photodegradation. In contrast, the presence of Good's buffers significantly accelerated MO removal, but the removal rate varied for different buffers. After irradiation for 90 min, the MO was depleted in the treatment with TRIS, but only 32% MO removal was achieved in PIPES treatment.

Previous studies have shown that hydroxyl group, especially when present as multidentate ligand, could promote LMCT.[15, 16] This was confirmed by our results where the buffers with hydroxyl group (i.e., TAPS, TRIS and HEPES) all exhibited higher MO removal than those without hydroxyl groups (i.e., PIPES and MOPS). In addition, addition of methanol, which contains hydroxyl groups but without pH buffering capability, significantly enhanced MO degradation, further confirming that antenna molecules with hydroxyl group are conducive to LMCT excitation (Fig. S2).

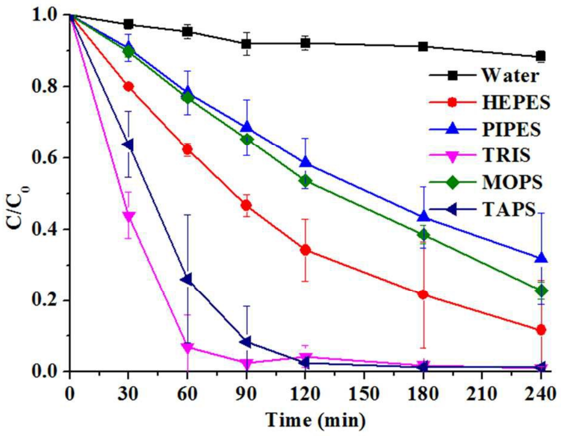

Fig. 1 Photodegradation of MO by LMCT excitation of TiO_2 with different Good's buffers under visible light irradiation.

Pathway of MO Photodegradation by TiO_2-HEPES complex

To better understand the roles of Good's buffers in LMCT excitation of TiO_2 for MO degradation, HEPES (with pH buffering range of 7.3~8.7) was chosen as a representative antenna molecular for in-depth investigation. Our results showed no obvious MO removal in the dark and in the treatments with HEPES alone (Fig. 2A), indicating that MO was removed by photodegradation but photosensitization was not the main route. The TiO_2 alone system showed only slight MO degradation, because TiO_2 with wide band gap could not be excited by visible light. In contrast, the co-presence of HEPES and TiO_2 led to rapid degradation of MO. The adsorption spectra (Fig. 2B) shows that the characteristic

View Article Online
DOI: 10.1039/C6RA02979E

Table 1 List of biological buffers used in this study.

Name	Abbreviation	Structure	pKa (25°C)
Piperazine-1,4-bisethanesulfonic acid	PIPES		6.96
3-Morpholinopropanesulfonic acid	MOPS		7.18
4-(2-Hydroxyethyl)-1-piperazineethanesulfonic acid	HEPES		7.56
Tris(hydroxymethyl) aminomethane	TRIS		8.07
[(2-Hydroxy-1,1-bis(hydroxymethyl)ethyl)amino]-1-propanesulfonic acid	TAPS		8.44

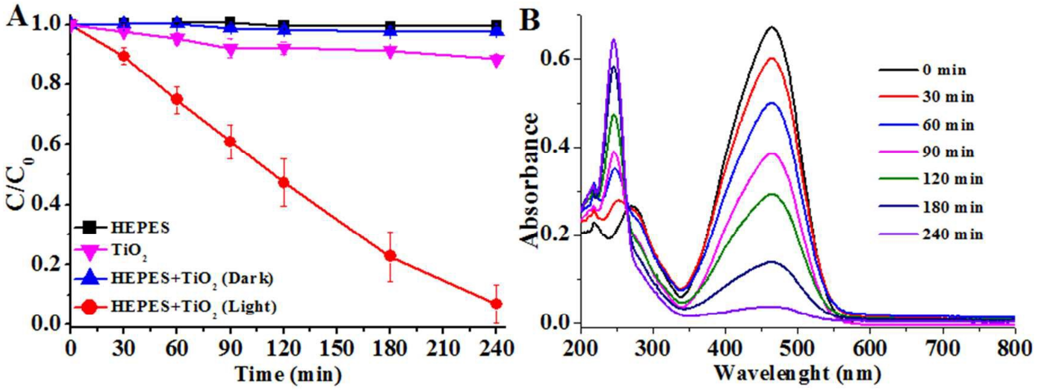

Fig. 2 Visible light photodegradation of MO by TiO_2 (0.5 g L^{-1}) in the presence of 50 mM HEPES at pH =7.0. (A), Photodegradation process of different treatments for 240 min; (B), Absorption spectra changes of the MO solution during photodegradation.

absorption peak of MO at 464 nm rapidly decreased over time, coupled with an arising new peak at 247 nm, indicting the cleavage of the azo bond[22-24] and formation of sulfanilic acid.[25]

The degradation products were further confirmed by GC-MS analysis. As shown in Fig. 3A, degradation products displayed a distinct peak at 9.78 min, which was identified as *N,N*-dimethylbenzene-1,4-diamine (Fig. 3B). Apparently, the azo bond of MO was broken to form amino group. The other degradation product of MO, 4-aminobenzenesulfonic acid, was not detected in this condition, because its intense hydrophilicity makes it difficult to be extracted by methylene chloride. Thus, the above results indicate that HEPES played an essential role in the process of TiO_2-catalyzed MO photodegradation under visible light, and the degradation occurred through a reduction pathway.

View Article Online
DOI: 10.1039/C6RA02979E

Since TiO_2 alone could not be excited by visible light, the visible light adsorption of TiO_2-HEPES complex should be attributed to the HEPES molecules that are adsorbed on the surface of TiO_2. This was validated by the DRS spectra results. As shown in Fig. 4, neither HEPES nor TiO_2 alone showed visible light response, but the HEPES-TiO_2 complex exhibited obvious visible light absorbance at 400~650 nm. This result indicates the formation of charge-transfer-complex (CTC) between TiO_2 and HEPES,[17] which contributed to the enhanced degradation of MO in our study.

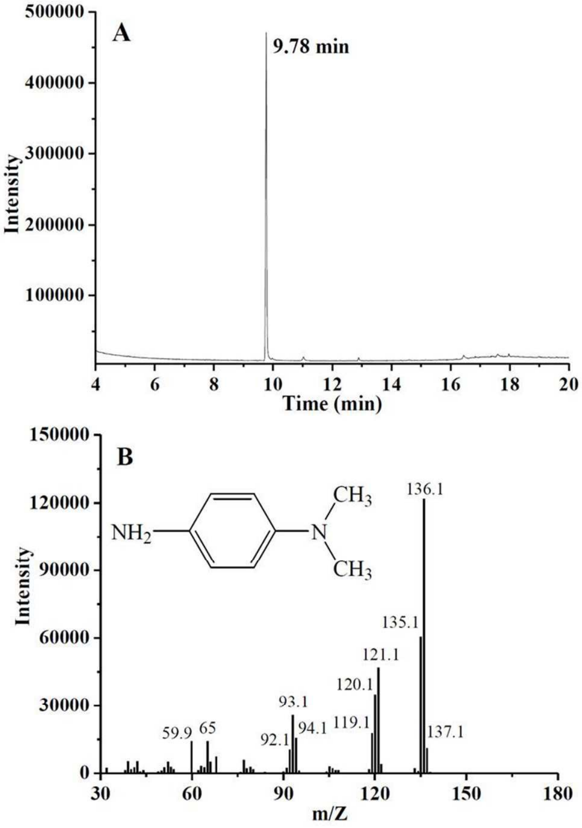

Fig. 3 GC chromatogram of the degradation products of MO in HEPES solution (A) and the MS fragmentation pattern at the time 9.78 min (B).

To validate that MO photodegradation under visible light was indeed driven by LMCT and to elucidate the degradation pathway, Cr(VI) and AO were used as the scavengers of e^- and h^+, respectively. As shown in Fig. 5, addition of AO inhibited the degradation of MO slightly, indicating that h^+ had no remarkable contribution to the MO degradation. A competition between AO and HEPES for the adsorption sites on TiO_2 surface might also contributed to the suppression.

In contrast, the MO degradation was completely inhibited in the presence of Cr(VI), indicating that the excited e^- played a key role in the azo-bond cleavage. These results confirm that the degradation of MO in TiO_2-HEPES was mediated by LMCT process via a reductive pathway.

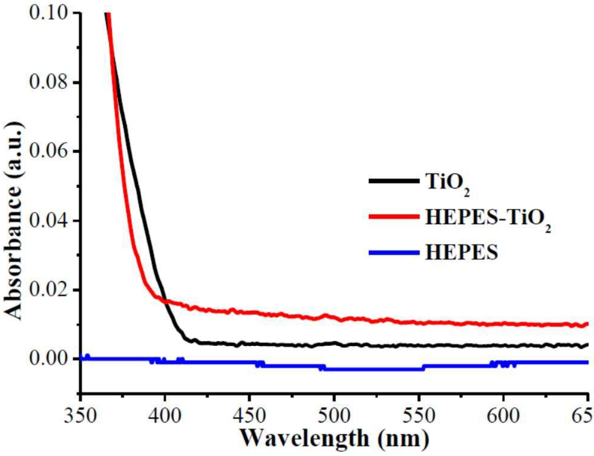

Fig. 4 UV-vis diffuse reflectance spectra of HEPES, TiO_2 and TiO_2-HEPES complex.

Based on the above results, we propose the following pathways of enhanced MO photodegradation by TiO_2 in presence of HEPES. HEPES as an antenna molecule is first absorb on the surface of TiO_2 to form TiO_2-ligand complex; Under visible light irradiation, photoelectrons are excited on the TiO_2-HEPES surface complexes and then transferred to the conduction band (CB) of TiO_2;[12, 26] MO molecules are then reduced by the photoelectrons on the surface of TiO_2-HEPES complex,[27, 28] forming 4-aminobenzenesulfonic acid and *N*,*N*-dimethylbenzene-1,4-diamine (Fig. S3).

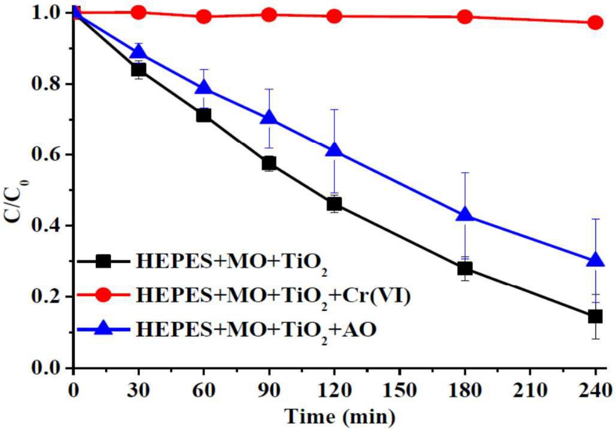

Fig. 5 Effect of 1 mM scavengers of h^+ and e^- on the MO photodegradation (C_{HEPES}=50 mM).

Mechanisms of LMCT excitation of TiO_2 by HEPES

Our results showed that the hydroxyl group of HEPES played an important role in LMCT excitation of TiO_2 for enhanced photodegradation (Fig. 1 and Fig. 2A). Thus, it can be expected that a higher concentration of HEPES would accelerate the degradation of MO because more hydroxyl groups become available. This was validated by our tests with different HEPES concentrations at a

View Article Online
DOI: 10.1039/C6RA02979E

constant pH of 7.0 (Fig. 6A). Thus, raising the HEPES concentration led to formation of more TiO_2-ligand complex and a higher visible light photodegradation activity. The excess of HEPES may also alter the zero point potential of TiO_2 and enhance its binding with MO,[17] thereby further improving the MO degradation.

The molecule structure of HEPES may also affect its binding with TiO_2 and thus the photodegradation activity. Since the solution pH poses influences on the molecular structure of HEPES, it is also supposed to affect MO photodegradation by TiO_2-HEPES complex. As expected, our results showed an obviously negative correlation between solution pH value and the MO photodegradation efficiency (Fig. 6B). With decreasing pH, the MO removal was improved gradually and the maximum degradation rate was achieved at pH 6.5. This increased photodegradation activity at acidic pH may be associated with the pronation of HEPES molecules, forming an acid structure with more hydroxyl groups that can readily form charge transfer complex with TiO_2 and induce visible light excitation of the LMCT process.[29]

A consistent result can be seen from the comparison of different buffers. In general, there was an good positive correlation between the MO removal efficiencies at pH 7.0 and the pKa values of different Good's buffers except for TRIS (Fig. 1). With increasing pKa value of the buffer in the order of PIPES, MOPS, HEPES and TAPS, the MO photodegradation rate increased accordingly due to the formation of conjugate acid structure that is more conducive to electronic excitation by LMCT than conjugate base structure. Interestingly, the TiO_2-TRIS complex showed the highest LMCT activity and the fastest MO photodegradation despite of its slightly lower pKa value than TAPS. This extraordinary performance of TRIS might be attributed to its highest number of hydroxyl groups and the influence of amine functional group. Like the hydroxyl group, the amine groups can also complex with TiO_2 and contribute to LMCT, but is less effective than hydroxyl group. Thus, as the amine functional groups become protonated (at pH lower than pKa), the nitrogen-metal interaction would be diminished, which causes less competition for hydroxyl group to access the TiO_2 and hence improves the formation of more effective complex for LMCT (Fig. S4). The superior degradation performance of TAPS over TRIS might be due to its different amino group structure that favours a more efficient LMCT process.

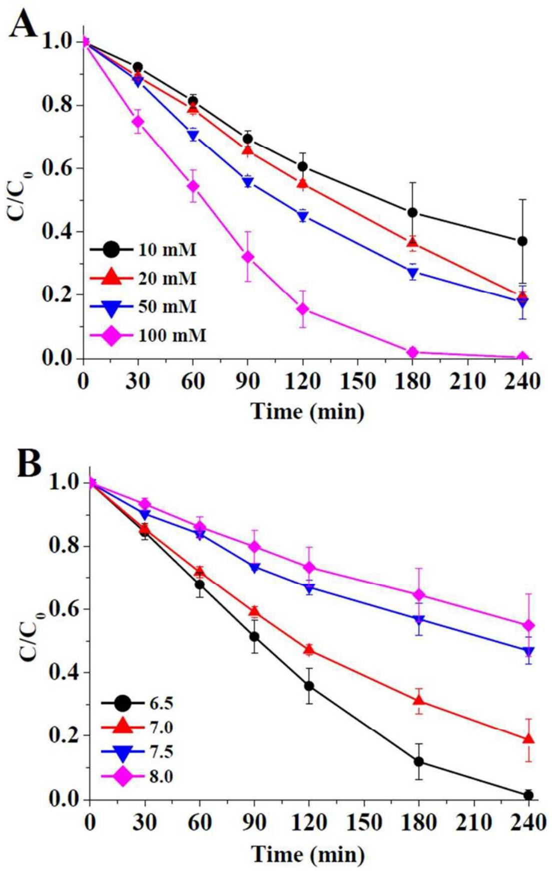

Fig. 6 MO photodegradation by TiO_2-HEPES at different buffer concentration (A) and pH (B).

Implications

Given the significant influences of pH on the LMCT activity, our results also suggest that the good pH buffer capability of Good's buffer could bring extra benefits by maintaining a favourable pH condition for TiO_2-based photocatalytic reactions.

In addition, the findings in this study imply that the potential influences of various soluble organic matters (DOMs) in natural aquatic environment (many of them possess hydroxyl functional groups) should be paid attention. A better understanding and utilization of the LMCT roles of such DOMs may lead to development of more efficient photocatalytic remediation process.

Conclusions

This study demonstrates that Good's buffers could be used as effective antenna molecules to induce visible light photocatalytic activity of TiO_2 through LMCT excitation. HEPES, as a typical Good's buffer, was found to complex with TiO_2. Under visible light irradiation, electrons were excited from the TiO_2-HEPES complex through LMCT process and transferred to the conduction band of TiO_2, leading to reductive degradation of MO. The LMCT activity of Good's buffers was strongly dependent on their molecule structure, especially the states of hydroxyl and amino groups. These functional groups varied with the concentration and type of adopted buffer and was significantly affected by solution pH. LMCT excitation was favoured by a conjugate acid structure of the buffers with the presence of more hydroxyl function and was affected by the amino group. This study broadens our knowledge of LMCT and has valuable implications for development of more efficient photocatalytic remediation process.

Acknowledgements

This study was partially supported by National Natural Science Foundation of China (51478208, 51278479, 51522812, 51538012)

View Article Online
DOI: 10.1039/C6RA02979E

and the Collaborative Innovation Center of Suzhou Nano Science and Technology of the Ministry of Education of China.

Notes and references

1. A. Fujishima, *Nature*, 1972, **238**, 37-38.
2. M. Koelsch, S. Cassaignon, C. Ta Thanh Minh, J. F. Guillemoles and J. P. Jolivet, *Thin Solid Films*, 2004, **451**, 86-92.
3. A. Amtout and R. Leonelli, *Phys. Rev. B*, 1995, **51**, 6842-6851.
4. R. Asahi, Y. Taga, W. Mannstadt and A. Freeman, *Phys. Rev. B*, 2000, **61**, 7459-7465.
5. S. G. Kumar and L. G. Devi, *J. Phys. Chem. A*, 2011, **115**, 13211-13241.
6. A. Fujishima, X. T. Zhang and D. A. Tryk, *Surf. Sci. Rep.*, 2008, **63**, 515-582.
7. Y. C. Hsiao, T. F. Wu, Y. S. Wang, C. C. Hu and C. Huang, *Appl. Catal. B*, 2014, **148-149**, 250-257.
8. A. L. Linsebigler, G. Lu and J. T. Yates Jr, *Chem. Rev.*, 1995, **95**, 735-758.
9. S. Higashimoto, N. Kitao, N. Yoshida, T. Sakura, M. Azuma, H. Ohue and Y. Sakata, *J. Catal.*, 2009, **266**, 279-285.
10. X. J. Lang, W. H. Ma, C. C. Chen, H. W. Ji and J. C. Zhao, *Accounts Chem. Res.*, 2013, **47**, 355-363.
11. X. J. Lang, W. H. Ma, Y. B. Zhao, C. C. Chen, H. W. Ji and J. C. Zhao, *Chem Eur J*, 2012, **18**, 2624-2631.
12. G. Zhang, G. Kim and W. Choi, *Energy Environ. Sci.*, 2014, **7**, 954-966.
13. N. Wang, L. H. Zhu, K. J. Deng, Y. B. She, Y. M. Yu and H. Q. Tang, *Appl. Catal. B*, 2010, **95**, 400-407.
14. N. E. Good, G. D. Winget, W. Winter, T. N. Connolly, S. Izawa and R. M. Singh, *Biochemistry*, 1966, **5**, 467-477.
15. T. Kamegawa, H. Seto, S. Matsuura and H. Yamashita, *ACS Appl. Mater. Interfaces*, 2012, **4**, 6635-6639.
16. S. Higashimoto, Y. Hatada, R. Ishikawa, M. Azuma, Y. Sakata and H. Kobayashi, *Curr. Org. Chem.*, 2013, **17**, 2374-2381.
17. G. Kim and W. Choi, *Appl. Catal. B*, 2010, **100**, 77-83.
18. T. Paul, P. L. Miller and T. J. Strathmann, *Environ. Sci. Technol.*, 2007, **41**, 4720-4727.
19. O. Carp, C. L. Huisman and A. Reller, *Prog. Solid State Ch.*, 2004, **32**, 33-177.
20. Y. X. Chen, S. Y. Yang, K. Wang and L. P. Lou, *J. Photochem. Photobiol. A*, 2005, **172**, 47-54.
21. L. S. Zhang, K. H. Wong, H. Y. Yip, C. Hu, J. C. Yu, C. Y. Chan and P. K. Wong, *Environ. Sci. Technol.*, 2010, **44**, 1392-1398.
22. H. Gao, S. Yan, J. Wang and Z. Zou, *Appl. Catal. B*, 2014, **158-159**, 321-328.
23. R. Comparelli, E. Fanizza, M. L. Curri, P. D. Cozzoli, G. Mascolo, R. Passino and A. Agostiano, *Appl Catal, B*, 2005, **55**, 81-91.
24. P. J. Cai, X. Xiao, Y. R. He, W. W. Li, J. Chu, C. Wu, M. X. He, Z. Zhang, G. P. Sheng, M. H. Lam, F. Xu and H. Q. Yu, *Appl. Microbiol. Biotechnol.*, 2012, **93**, 1769-1776.
25. R. Comparelli, E. Fanizza, M. Curri, P. Cozzoli, G. Mascolo, R. Passino and A. Agostiano, *Appl. Catal. B*, 2005, **55**, 81-91.
26. N. Wang, L. Zhu, K. Deng, Y. She, Y. Yu and H. Tang, *Appl Catal, B*, 2010, **95**, 400-407.
27. F. Chen, Z. G. Deng, X. P. Li, J. L. Zhang and J. C. Zhao, *Chem. Phys. Lett.*, 2005, **415**, 85-88.
28. L. Cermenati, P. Pichat, C. Guillard and A. Albini, *J. Phys. Chem. B*, 1997, **101**, 2650-2658.
29. X. Lang, W. Ma, Y. Zhao, C. Chen, H. Ji and J. Zhao, *Chem. Eur. J.*, 2012, **18**, 2624-2631.

View Article Online
DOI: 10.1039/C6RA02979E

Graphical Abstract

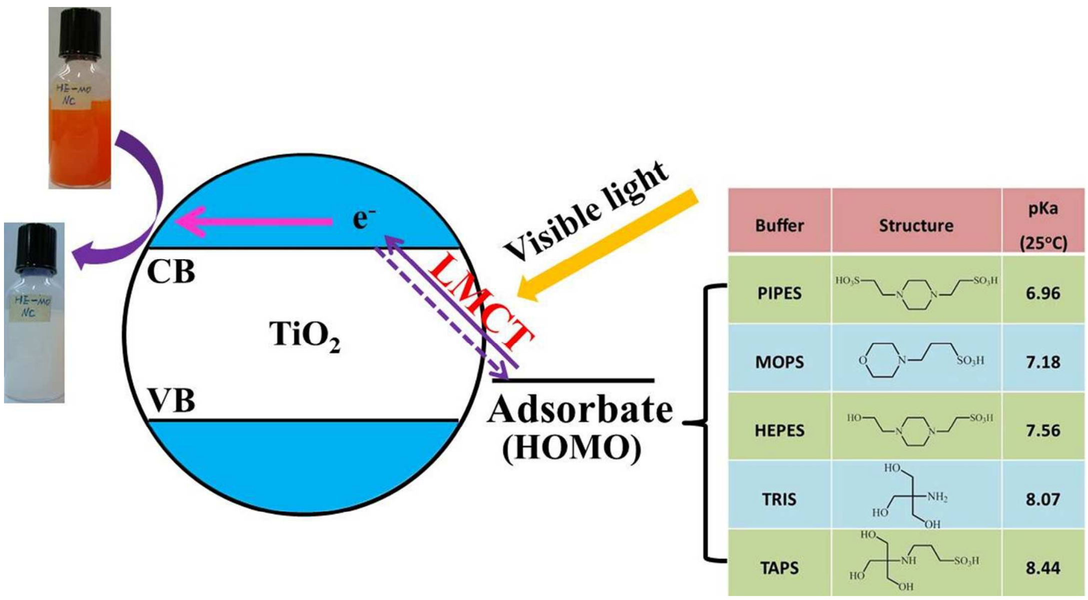

Buffer	Structure	pKa (25°C)
PIPES		6.96
MOPS		7.18
HEPES		7.56
TRIS		8.07
TAPS		8.44